Charge Transport and Storage in MetalNitrideOxideSilicon (MNOS) Structures

D. FrohmanBentchkowsky and M. Lenzlinger

Citation: J. Appl. Phys. **40**, 3307 (1969); doi: 10.1063/1.1658181
View online: http://dx.doi.org/10.1063/1.1658181
View Table of Contents: http://jap.aip.org/resource/1/JAPIAU/v40/i8
Published by the American Institute of Physics.

Charge Transport and Storage in Metal–Nitride–Oxide–Silicon (MNOS) Structures*

D. FROHMAN-BENTCHKOWSKY AND M. LENZLINGER

Fairchild Semiconductor, Research and Development Laboratory, 4001 Miranda Avenue, Palo Alto, California 94304

(Received 19 February 1969; in final form 31 March 1969)

A simple physical model that predicts charge accumulation at the dielectric interface of metal–nitride–oxide–silicon (MNOS) structures is proposed and verified experimentally. The model is based on the presence of steady-state current flow in the dielectric structure. Interface-charge accumulation is shown to be determined by the requirement for continuity of current through the structure under steady-state conditions. Continuity of current is established by accumulation of either positive or negative charge for a given polarity of charging voltage, depending on the relative current-field characteristics of the silicon nitride and silicon dioxide layers. Due to the exponential nature of the current–field characteristics, the time required to reach steady state is a strong function of the applied charging voltage. This leads to the observed charge storage property of MNOS devices. The hysteresis characteristic observed in MNOS structures is shown to be time-dependent with a tendency to merge into a single-valued dependence of accumulated charge on charging voltage as the steady-state condition is approached. The validity of the theoretical model for both steady-state and transient behavior is confirmed by current–voltage, capacitance–voltage, and turn-on measurements of MNOS capacitors and transistors for different dielectric thickness ratios and over a wide temperature range. The underlying concept that charge accumulation establishes current continuity in a two-layer dielectric structure should be valid, in general, for any two-dielectric structure.

I. INTRODUCTION

Metal–nitride–oxide–silicon (MNOS) devices have been shown to exhibit charge storage characteristics.[1] As a result, considerable interest has been expressed in their potential application as memory elements.[2] The memory function of these devices has been attributed to trapping of charge at the nitride–oxide interface. Consequently, it becomes important to understand charge transport mechanisms in MNOS structures. This paper will present a consistent model of charge transport and storage in MNOS structures.

Previous investigations have shown that steady-state current flows in both metal–oxide–silicon (MOS)[3] and metal–nitride–silicon (MNS)[4] structures. It is proposed that steady-state current also flows through the MNOS structure and that the charge trapped at the nitride–oxide interface is determined by the balance of the currents in the two dielectrics. Since the current-field characteristics are different for the two materials, the fields will tend to adjust themselves by charge accumulation at the interface until current continuity is established. On application of a positive voltage to the gate electrode, this model predicts the possibility of accumulation of either positive charge or negative charge at the nitride–oxide interface, depending on the conduction characteristics and thicknesses of the silicon nitride and silicon dioxide layers. Although the MNOS structure is used as a reference, the model is applicable to the general case of any two-dielectric structure.

The validity of the theoretical model is confirmed by current–voltage, capacitance–voltage, and turn-on measurements of MNOS capacitors and transistors for different dielectric conduction characteristics and over a wide temperature range. Current measurements are consistent with results previously published for conduction in both the silicon dioxide,[3] due to tunneling from the silicon into the oxide conduction band, and the silicon nitride,[4] due to excitation from traps into the silicon nitride conduction band. Both the conventional mode of device operation (accumulation of negative charge at the nitride–oxide interface for a positive applied voltage) and the inverse mode of operation (accumulation of positive charge at the nitride–oxide interface for a positive applied voltage) have been observed. Since current flow is predicted to persist down to very low applied voltage levels, the hysteresis characteristic observed in MNS and MNOS structures should merge into a single line if true steady state is obtained, i.e., if the voltages are applied for a long period of time (hours and days). This tendency has been confirmed experimentally on all structures investigated.

II. CONDUCTION IN SILICON DIOXIDE AND SILICON NITRIDE

Consider an MNOS structure as shown in Fig. 1. The variation of the energy bands with distance in a direction normal to the surface, for positive and negative bias on the metal electrode with respect to the semiconductor substrate, is illustrated in Fig. 2. An investigation of charge transport and storage in this structure requires an understanding of conduction mechanisms in MOS and MNS structures. Results of studies on these structures have been reported.[3,4]

The dominant current-transport mechanism in MOS structures was shown to be electrode-limited due to

---

* This paper was presented at the IEEE International Electron Devices Meeting, Washington, D.C., October 1968.

[1] H. C. Pao and M. O'Connell, Appl. Phys. Lett. **12**, 260 (1968).

[2] H. A. R. Wegener *et al.*, "The Variable Threshold Transistor, a New Electrically-Alterable, Nondestructive Read-Only Storage Device," IEEE Int. Electron Devices Meeting, Washington, D.C., October 1967.

[3] M. Lenzlinger and E. H. Snow, J. Appl. Phys. **40**, 278 (1969).

[4] S. M. Sze, J. Appl. Phys. **38**, 2951 (1967).

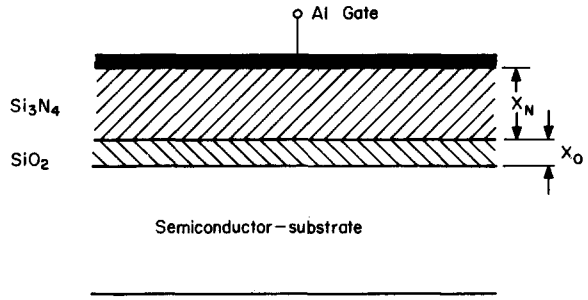

FIG. 1. Cross section of MNOS structure.

Fowler–Nordheim emission given by the following expression[3]:

$$J_0 = C_0 E_0^2 \frac{\pi ckT/E_0}{\sin(\pi ckT/E_0)} \exp\left(\frac{-E_1}{E_0}\right), \qquad (1)$$

where E_0 is the electric field in the oxide, T is the temperature in °K, k is Boltzmann's constant, and E_1, C_0, c are characteristic constants depending on the barrier height of the interface. The temperature dependence of the Fowler–Nordheim current stems from the dependence on temperature of the number of electrons of a given energy incident on the barrier. The values of the constant terms in the current-density expression [Eq. (1)] for the oxide–silicon interface were found to be

$$C_0 = 10^{-5}\ \mathrm{A/V^2},$$

$$E_1 = 2.54\times10^{8}\ \mathrm{V/cm},$$

$$c = 1.12\times10^{27}\ (\mathrm{C\cdot cm})^{-1}.$$

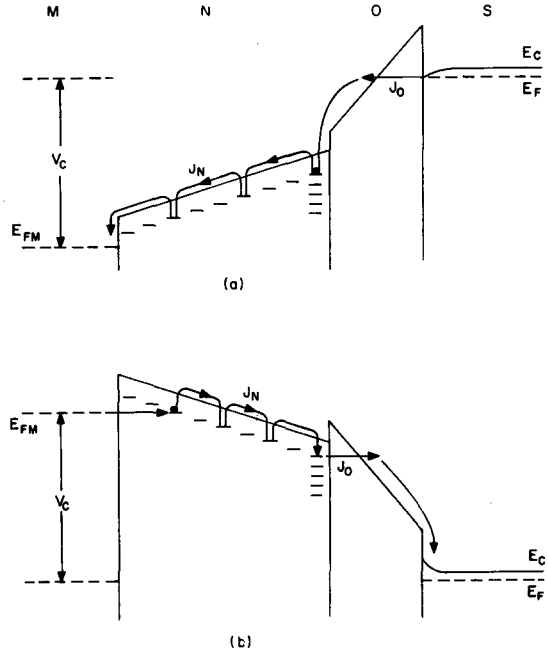

FIG. 2. Energy band diagram of MNOS structure under (a) positive bias and (b) negative bias.

When the thickness of the oxide is reduced to a value below which direct tunneling is possible from the semiconductor into the interface traps (<50 Å), the expression for the current component in the oxide (J_0) has to be modified to account for the change in the conduction mechanism from Fowler–Nordheim emission to direct tunneling.[5] This case has not been investigated in the present work. However, since the basic derivations of current transport in the MNOS structure are independent of the specific current mechanism in the oxide or the nitride, the model applies, in principle, to a structure which allows direct tunneling through the oxide.

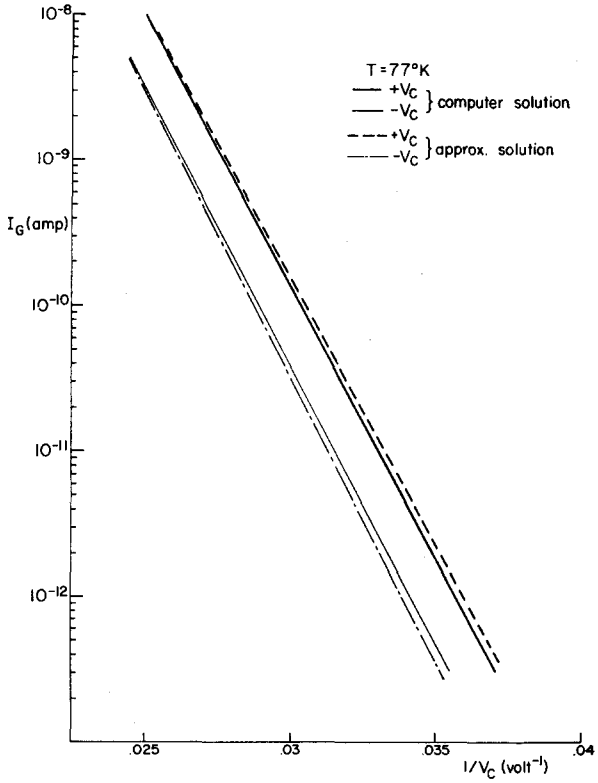

FIG. 3. Current as a function of charging voltage at low temperatures. $x_0 = 50$ Å, $x_n = 500$ Å, area $= 1.3\times10^{-4}$ cm².

In MNS structures current transport was shown to be bulk-limited due to Schottkye mission from traps above room temperature and field emission (tunneling) from the same traps into the silicon nitride conduction band at low temperatures. At low fields there is an additional ohmic component. The current-density expression consists of three terms:[4]

$$J_n = J_{n1} + J_{n2} + J_{n3}. \qquad (2)$$

J_{n1} corresponds to field-enhanced thermal excitation (Poole–Frenkel effect) and is given by

$$J_{n1} = C_1 E_n \exp(-q\phi_1/kT) \exp[(q/kT)(\beta E_n)^{1/2}], \qquad (3)$$

[5] J. Shewchun, A. Waxman, and G. Warfield, Solid-State Electron. **10**, 1165 (1967).

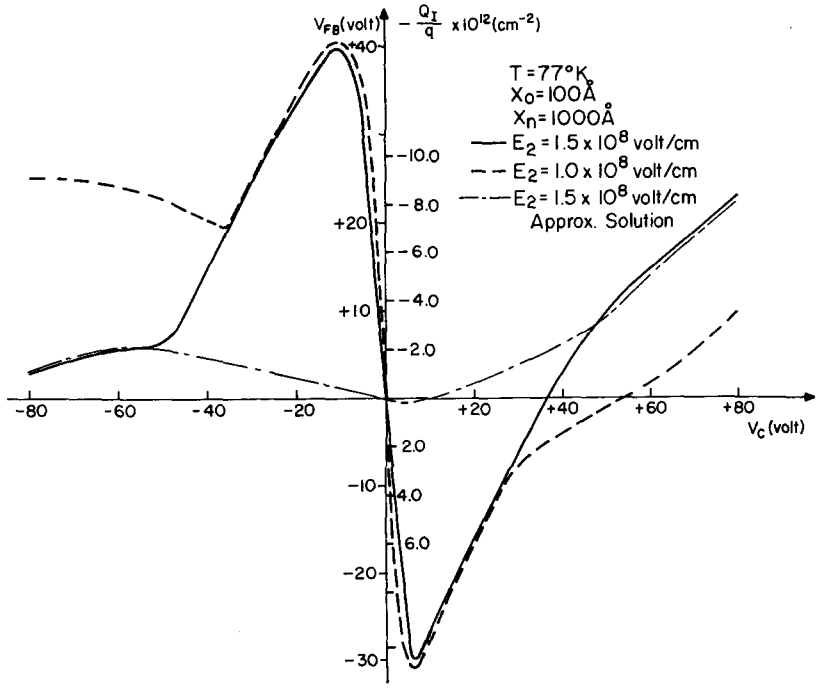

FIG. 4. Equilibrium induced interface charge as a function of charging voltage at low temperature for two values of E_2. The dot-dashed line represents the approximate solution for $E_2=1.5\times10^8$ V/cm.

where E_n is the electric field in the nitride, ϕ_1 is the depth of the trap-potential well, and C_1, β are characteristic constants depending on the trap level and the dielectric constant. J_{n2} is due to field emission of trapped electrons into the dielectric conduction band:

$$J_{n2}=C_2E_n^2\exp(-E_2/E_n). \tag{4}$$

E_2 and C_2 are characteristic constants depending on the trap level. J_{n3} results from hopping of thermally excited electrons between isolated trapping states.[6]

$$J_{n3}=C_3E_n\exp(-q\phi_3/k\mathrm{T}), \tag{5}$$

where $q\phi_3$ is the thermal activation energy.

The values of the constant terms in these current-density expressions for silicon nitride were found to be as follows:

$C_1=3.0\times10^{-9}$ A/V·cm, $\quad\phi_1=1.0\pm0.2$ V,

$C_2=3.5\times10^{-10}$ A/V^2, $\quad E_2=1.2\times10^8$ V/cm,

$C_3=5.0\times10^{-14}$ A/V·cm, $\quad\phi_3=0.1$ V,

$\beta=1.18\times10^{-7}$ V·cm.

The deviation from the values reported in Ref. 4 is due to a difference in deposition conditions affecting the characteristic constants of the current-density expressions. In the derivations that follow, the values of the constants listed above (for the oxide and the nitride) will be assumed unless otherwise specified.

[6] N. F. Mott and W. D. Twose, Advan. Phys. 10, 107 (1961).

III. CONDUCTION AND STORAGE IN MNOS STRUCTURES

Based on the results in Sec. II, it is expected that current will flow in the MNOS structure (Fig. 1) on application of a bias voltage to the metal electrode. Figure 2(a) depicts the case of a positive metal electrode or gate voltage with respect to the semiconductor substrate. In this case the steady-state current consists of electrons tunneling from the semiconductor into the oxide conduction band, dropping into traps at the nitride–oxide interface, and being excited in turn into the nitride conduction band to the metal electrode. This corresponds to the current-transport mechanisms described in Eqs. (1) and (2), respectively. The description is limited to electron transport since evidence of hole transport in this structure has not been reported and no evidence for it has been found in this investigation. For the case of a negative metal bias [Fig. 2(b)], the steady-state current will similarly consist of electrons, which are excited from traps into the silicon nitride conduction band, tunneling through the nitride–oxide barrier into the oxide and semiconductor conduction band. Note that conduction in this case involves electron transport through the nitride–oxide interface barrier. It is assumed here that the transport mechanism is Fowler–Nordheim tunneling from the silicon nitride into the silicon dioxide conduction band. (The transport mechanism in this case could also be due to hole emission from the silicon into the silicon dioxide valence band. However, the two mechanisms could not be distinguished experimentally.) Consequently, Eq. (1) should apply with different values for C_0 and E_1:

$$J_{0-}=C_{0-}E_0^2\exp(-E_{1-}/|E_0|). \tag{6}$$

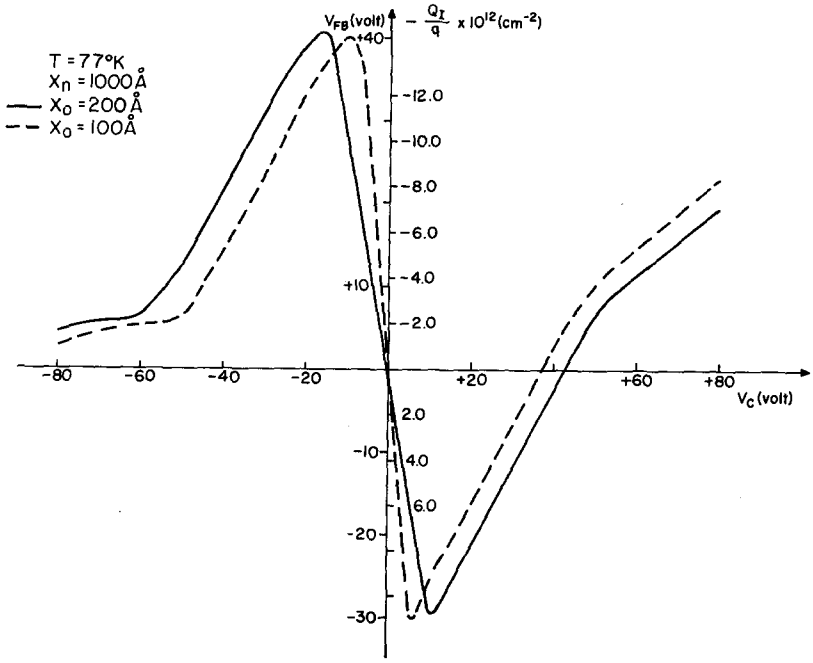

FIG. 5. Equilibrium induced interface charge as a function of charging voltage at low temperature for two values of oxide thickness.

Since the energy-barrier height of this interface has not been determined previously, the values of C_{0-} and E_{1-} were obtained from experimental measurements at low temperatures on MNOS structures, resulting in

$$C_{0-}=9.0\times10^{-8}\ \text{A/V}^2,$$

$$E_{1-}=3.2\times10^{8}\ \text{V/cm}.$$

Because in this case the temperature dependence of the number of carriers available for tunneling is not known, no temperature dependence was assumed for J_{0-}.

On application of a charging gate voltage (V_G), the fields in the oxide and the nitride (E_0, E_n) are determined initially by the dielectric constant ratio of the two dielectrics. The buildup of current through the structure will depend on the current–field characteristics of the nitride [Eq. (2)] and the oxide [Eq. (1)]. These characteristics, being different, result in a non-

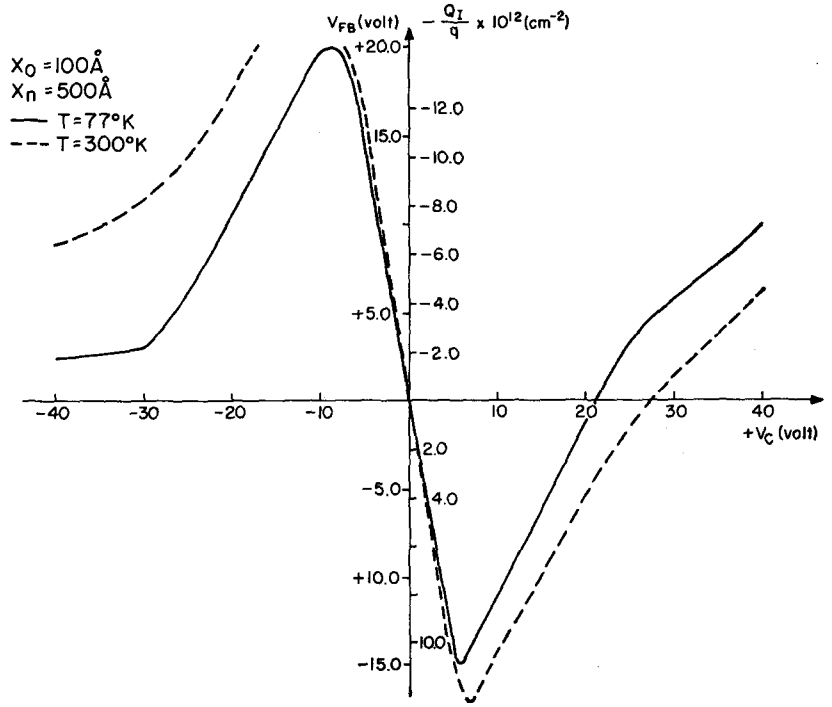

FIG. 6. Temperature dependence of equilibrium induced interface charge as a function of charging voltage.

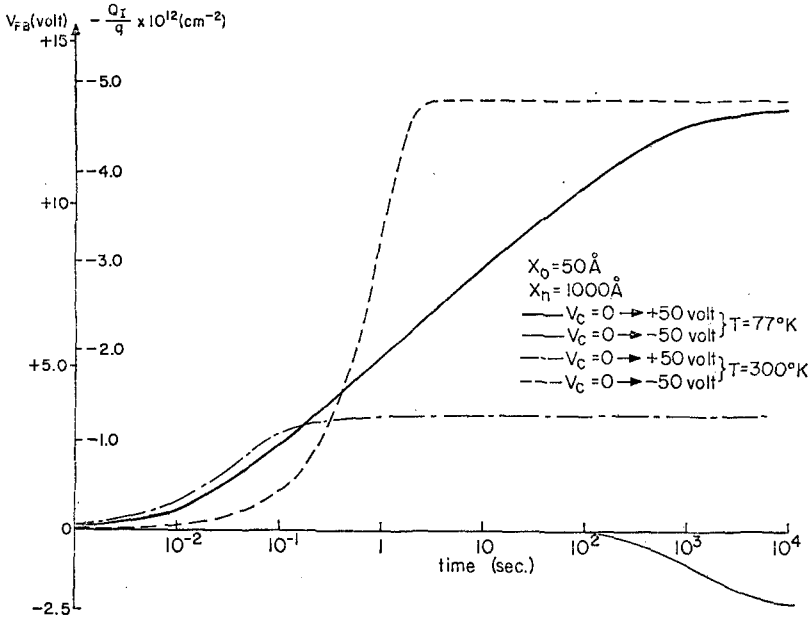

FIG. 7. Induced interface charge as a function of charging time for liquid nitrogen and room temperature.

equilibrium current discontinuity across the dielectric interface. The current discontinuity leads to charge accumulation at the interface, which in turn adjusts the electric field distribution until current continuity is established. This observation leads naturally to the steady-state and transient solutions for both the current and the charge. Note that the description of the interface trapping levels is only qualitative. The steady-state and transient solutions for charge transport in the MNOS structure do not require knowledge of the exact trap distribution.

A. Steady-State Analysis

The steady-state solution will consist of a determination of the electric fields in the two dielectrics (E_0, E_n) and the charge accumulated at the dielectric interface (Q_I). Current continuity in the steady state requires that for a given applied voltage

$$J_0 = J_n. \tag{7}$$

Continuity of the electric flux leads to

$$K_0 E_0 - K_n E_n = Q_I/\epsilon_0, \tag{8}$$

where Q_I is the charge accumulation at the nitride–oxide interface, $K_0=3.9$ is the relative dielectric constant of silicon dioxide, K_n is the relative dielectric constant of silicon nitride (taken to be 6.5 unless otherwise specified), and ϵ_0 is the permittivity of free space. Summation of the potential drops across the structure results in

$$V_G = E_0 x_0 + E_n x_n, \tag{9}$$

where V_G is the voltage of the metal electrode with respect to the silicon substrate.

Simultaneous solution of Eqs. (7)–(9) leads to expressions for charge accumulation at the dielectric interface and current density in terms of the applied voltage and the dielectric thicknesses. In order to gain insight into the trends of the solution as a function of different parameters, the solution will be demonstrated at low temperatures. The similarity and relative simplicity of the oxide and the nitride current expressions in this temperature range [Eqs. (1) and (4)] allow for the derivation of closed-form expressions for current density and induced interface charge. Substitution of Eqs. (1) and (4) into Eq. (7) yields the current continuity in terms of the electric fields at low temperatures

$$C_0 E_0^2 \exp(-E_1/|E_0|) = C_2 E_n^2 \exp(-E_2/|E_n|). \tag{10}$$

To obtain a relatively simple solution, let us make the following assumptions (generally satisfied for the range

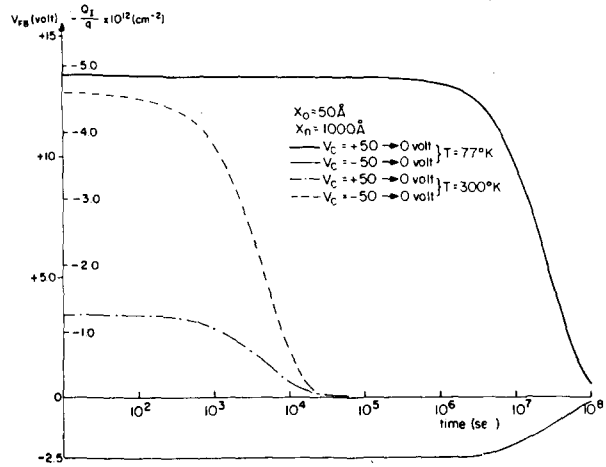

FIG. 8. Discharge of induced interface charge as a function of time for liquid nitrogen and room temperature.

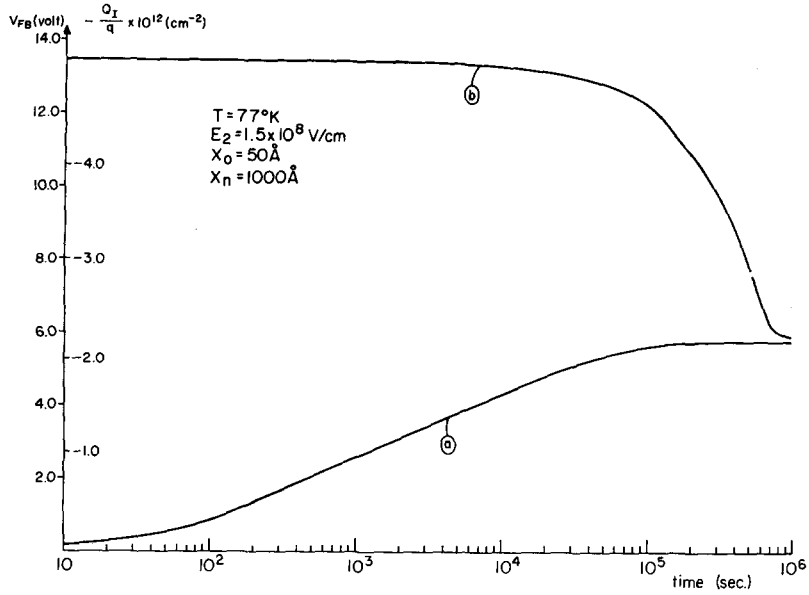

FIG. 9. Induced interface charge as a function of time for a given charging voltage ($V_C=+40$ V) and two values of initial interface charge $[Q_I(0)/q]$. (a) $Q_I(0)/q=0$. (b) $Q_I(0)/q=-5.0\times 10^{12}$ cm^{-2}.

of practical interest):

$$\text{(a)}\quad E_2x_n \gg E_1x_0, \qquad C_0 \geq C_2,$$

$$\text{(b)}\quad \ln(E_0^2/E_n^2) \ll \ln(C_0/C_2).$$

Under these assumptions the simultaneous solutions of Eqs. (8)–(10) yield the following expression for the charge accumulated at the dielectric interface:

$$Q_I=\left[\frac{\epsilon_0K_0E_1}{\alpha\mid V_C\mid+x_0E_1+x_nE_2}-\frac{\epsilon_0K_nE_2}{x_0E_1+x_nE_2}\right]V_C, \qquad (11)$$

where

$$\alpha=\ln(C_0/C_2)$$

for positive V_C. For negative V_C

$$\alpha=\ln(C_{0-}/C_2),$$

and E_{1-} is substituted for E_1. The electric fields are given by

$$E_0=E_1V_C/(\alpha\mid V_C\mid+x_0E_1+x_nE_2), \qquad (12)$$

$$E_n=E_2V_C/(x_0E_1+x_nE_2). \qquad (13)$$

Substitution of the electric field in Eq. (10) results in the current-density expression

$$\mid J_0\mid=\mid J_n\mid=C_n\left[\frac{E_2V_C}{x_0E_1+x_nE_2}\right]^2\exp\left[-\frac{x_0E_1+x_nE_2}{\mid V_C\mid}\right]. \qquad (14)$$

Solutions for the current density as a function of applied voltage for a typical structure, based on Eq. (14), are shown in Fig. 3. The results for both positive and negative charging voltages are compared with computer

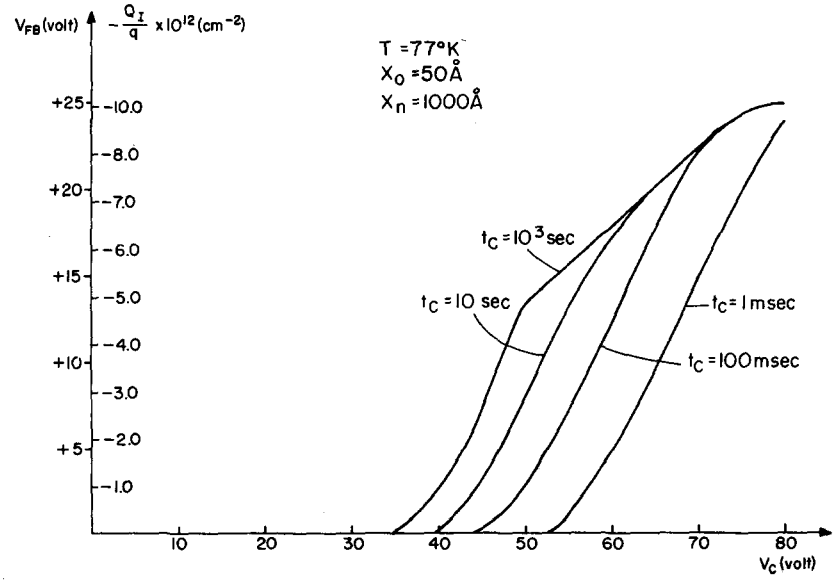

FIG. 10. Induced interface charge as a function of charging voltage for different values of charging time $[Q_I(0)=0]$.

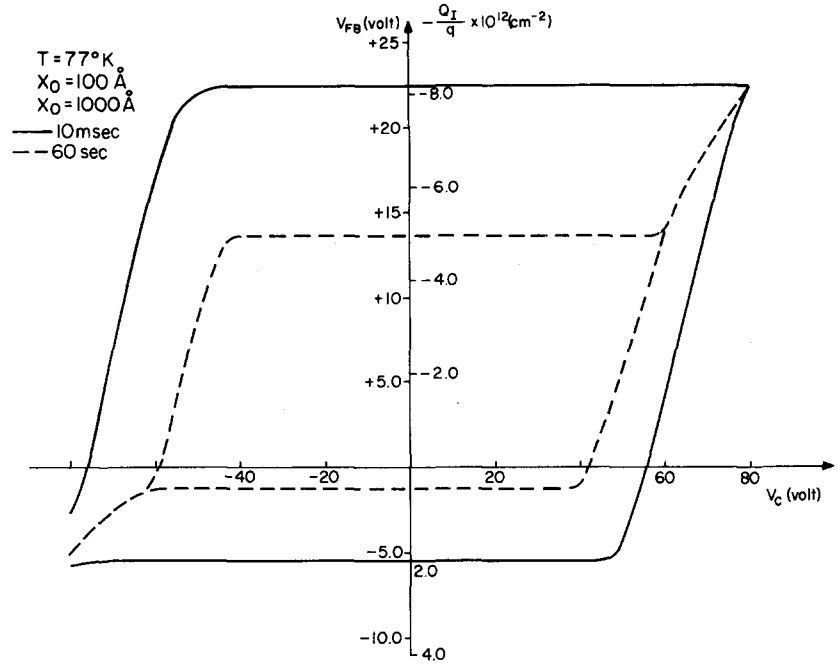

FIG. 11. Hysteresis behavior of induced interface charge as a function of charging voltage for two values of charging time. $V_{C\,min} = -80$ V, $V_{C\,max} = +80$ V, $\Delta V_C = 5$ V.

solutions based on Eqs. (7)–(9). Agreement between the solutions is good since the simplifying assumptions (a) and (b) are satisfied. Hence, Eq. (11) can be used to determine the accumulated charge dependence on the current–field characteristics and thickness of the dielectrics.

1. *Dependence of charge accumulation (Q_I) on the current-field characteristics and thickness of the dielectrics.* Equation (11) reflects the strong dependence of charge accumulation at the silicon nitride-silicon dioxide interface on the characteristic parameters (E_1, E_2) of the current-field relationships [Eqs. (1) and (4)] for the dielectrics. For a fixed dielectric thickness ratio (x_0/x_n) and a given applied voltage, it predicts accumulation of either positive or negative charge at the interface, depending on the relative magnitude of these characteristic parameters. If we assume the initial nitride-oxide interface charge density to be zero and define the initial dielectric currents J_{00}, J_{n0} under the condition of no induced charge at the interface [$Q_I(V_C) = 0$]

$$J_{00} = J_0(Q_I = 0),$$
$$J_{n0} = J_n(Q_I = 0), \qquad (15)$$

then the polarity of the induced charge is determined by the difference between the initial current densities $J_{n0}(V_C) - J_{00}(V_C)$. The charge at the silicon dioxide–silicon interface does not affect the field distribution in the dielectrics. A fixed charge[7] Q_{ss} at this interface will result in a constant shift of the flatband voltage equal to

$$\Delta V_{FB} = -(Q_{ss}/\epsilon_0)[(x_n/K_n) + (x_0/K_0)].$$

[7] A. S. Grove, B. E. Deal, E. H. Snow, and C. T. Sah, Solid-State Electron. **8**, 145 (1965).

In the following theoretical calculation the silicon dioxide–silicon interface charge is assumed to be zero.

To illustrate the dependence of induced interface charge on the characteristic conduction parameters of the dielectrics, the accumulated charge is plotted as a function of charging voltage at low temperature for two values of E_2 (Fig. 4); negative charge corresponding to a positive flatband voltage $V_{FB} = -x_n Q_I/K_n\epsilon_0$ is plotted in the positive direction of the ordinate. At large voltages ($|V_C| > 40$ V) Eq. (11) is in good agreement with computer solutions based on Eqs. (1), (2), and (7)–(9). A decrease in the value of E_2, and consequently an increase in the value of J_{n0} with respect to J_{00}, leads to a more positive accumulated charge for positive applied voltages and to the opposite tendency for negative voltages. At low voltages the current in the nitride is dominated by the ohmic component J_{n3} [Eq. (5)], which is not taken into account in the derivation of Eq. (11). The deviation resulting from this increase in the nitride current is again in the direction of more positive charge for positive applied voltages.

So far we have assumed a fixed dielectric thickness ratio (x_0/x_n). A variation in this ratio will clearly lead to a modification of the electric field distribution. This in turn will result in a variation of the induced charge for a given charging voltage. Solutions including the ohmic component J_{n3} are shown in Fig. 5. In agreement with Eq. (11), an increase in the oxide thickness leads to a more positive interface charge for large positive charging voltages.

2. *Temperature dependence of Q_I.* So far we have restricted the discussion to low temperatures because of the relative simplicity of the current-field expression in

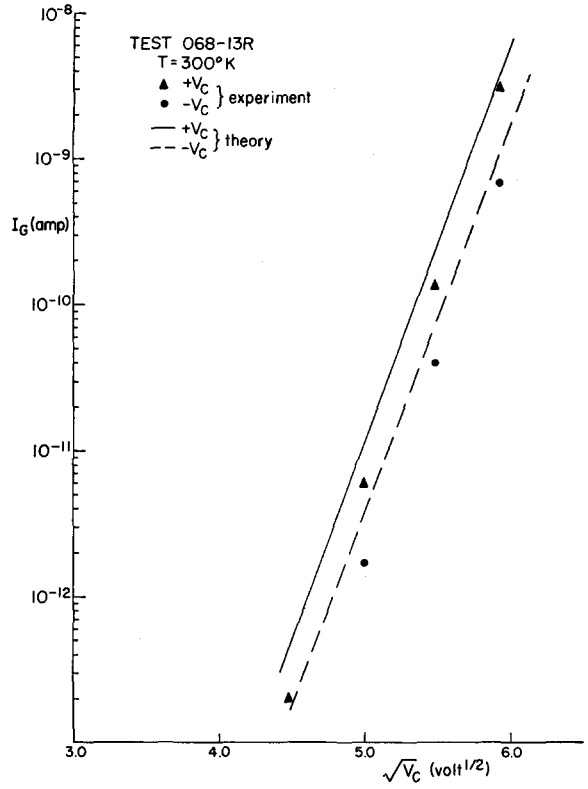

FIG. 12. Theory and experiment for the current as a function of $(V_C)^{1/2}$ at room temperature. $x_0=50$ Å, $x_n=530$ Å, area$=1.3\times10^{-4}$ cm^2.

this region. As the temperature is raised to room temperature and above, the change in relative magnitude of the current-density terms in Eqs. (1) and (2) will result in a modification of induced interface charge characteristics. At room temperature and above, the current density in the silicon nitride is dominated at moderate and high voltages by J_{n1} [Eq. (3)], and at low voltages by the ohmic component J_{n3} [Eq. (5)]. For silicon dioxide the temperature-dependent term in Eq. (1), which was negligible at low temperatures, also leads to an increase in current. However, the silicon nitride current increases more rapidly than the silicon dioxide current, due to the exponential temperature dependence of J_{n1}. The computer solution for induced charge as a function of applied charging voltage is shown in Fig. 6 and compared with the low-temperature solution for the same structure. As can be seen from a comparison of Figs. 4 and 6, the effect of higher temperature on the accumulated interface charge is in the same direction as the tendency observed for a lower value of E_2. This similarity is expected since the net result of both increased temperature and a lower value of E_2 is an increase of current density in the silicon nitride with respect to the silicon-dioxide component for the same applied voltage.

Finally, it should be noted that the charge-transport model predicts the induced charge in the steady state to be a single-valued function of the applied gate voltage. This implies that the MNOS device does not perform a memory function if operated under steady-state conditions. The reported charge storage characteristics[1,2,8,9] are due to the transient behavior to be discussed next.

B. Transient Analysis

The rate of change in interface charge will be directly proportional to the difference in current-density values for both dielectrics at a given charging voltage and time

$$dQ_I(V_C, t)/dt=J_0(V_C, t)-J_n(V_C, t). \quad (16)$$

The initial condition for induced interface charge at the nitride–oxide interface is determined by the past history of the device. The computer solutions of Eq. (16) for a given MNOS structure at both low and room temperatures are shown in Figs. 7 and 8. The charging-time dependence for both voltage polarities ($V_C=\pm50$ V) is illustrated in Fig. 7. Note the significant decrease in charging response time at room temperature due to the increased current levels. The time response of charge decay after the charging voltage is removed ($V_C=0$) is illustrated in Fig. 8. Again, the room-

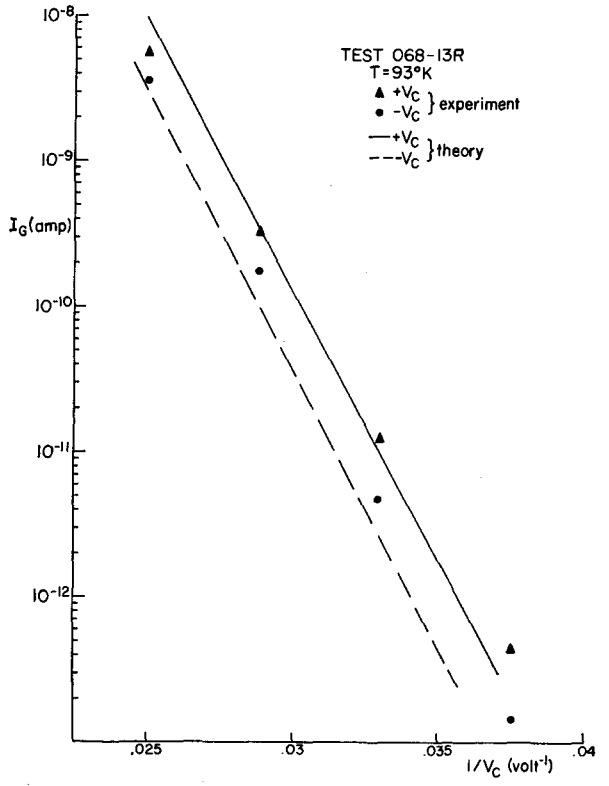

FIG. 13. Theory and experiment for the current as a function of $1/V_C$ at low temperature. $x_0=50$ Å, $x_n=530$ Å, area$=1.3\times10^{-4}$ cm^2.

[8] J. T. Wallmark and J. H. Scott, Jr., "Switching and Storage Characteristics of MIS Memory Transistors," IEEE Int. Electron Devices Meeting, Washington, D.C., October 1968.

[9] B. V. Keshavan and H. C. Lin, "MONOS Memory Element," IEEE Intern. Electron Devices Meeting, Washington, D.C., October 1968.

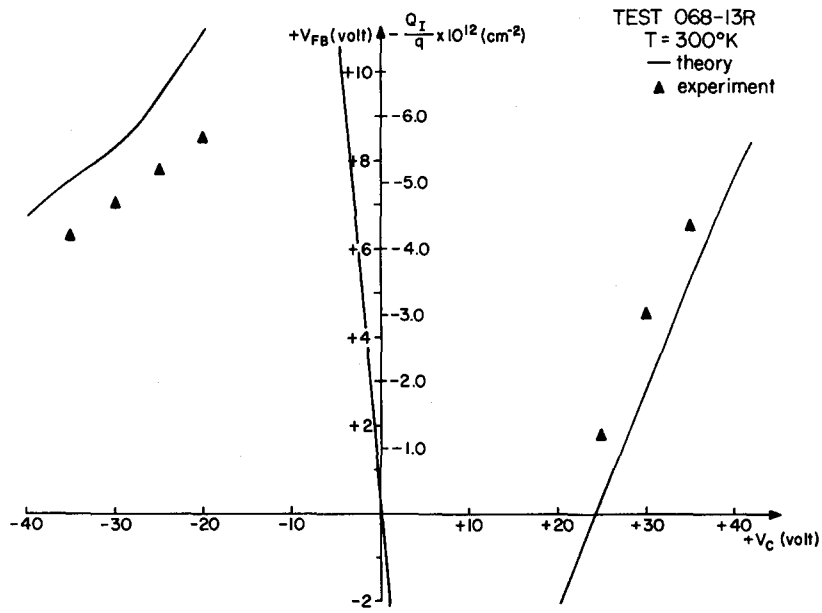

FIG. 14. Theory and experiment for the equilibrium induced interface charge as a function of charging voltage at room temperature. $x_0=50$ Å, $x_n=530$ Å.

temperature time response is faster due to the higher conduction level in the dielectrics. A comparison of Figs. 7 and 8 indicates that the charging time response is consistently a few orders of magnitude faster than the following discharge period under the same conditions. This results from a combination of the exponential nature of the current–field relationships for the dielectrics, and the lower average fields in the dielectrics during the discharge period as compared to the charging period. The time response difference is the key feature in practical applications of this structure as a memory element.

Hysteresis behavior of the time dependent Q_I vs V_C characteristics. It has been reported[10,11] previously that MNOS structures tend to exhibit hysteresis behavior. This implies that the induced interface charge is not a single-valued function of the charging voltage. From the above discussion, it becomes clear that the hysteresis behavior is a direct result of the finite duration of the applied charging voltage, which is not sufficient to achieve a steady-state condition, and the large difference between charging and discharging time responses. In Fig. 9 we demonstrate a solution of Eq. (16) for a positive charging voltage ($V_C=+40$ V) and two

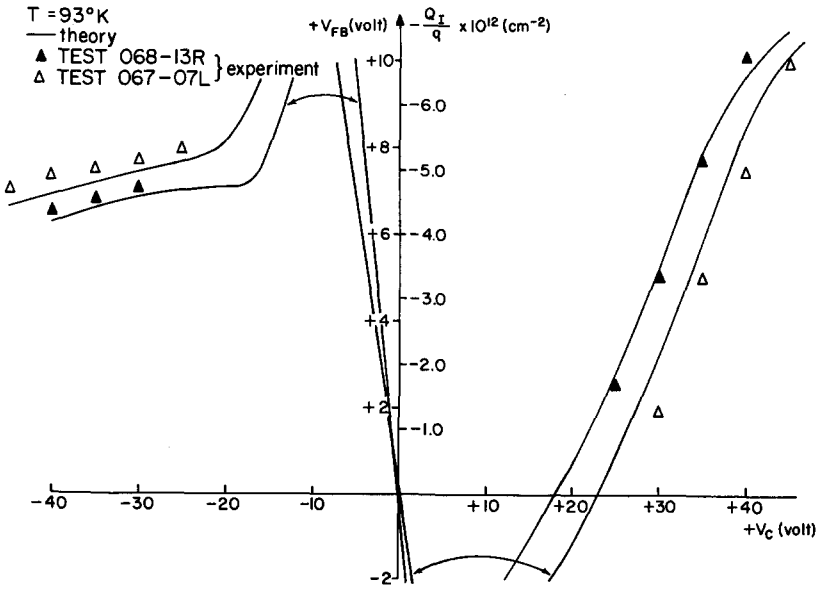

FIG. 15. Theory and experiment for the equilibrium induced interface charge as a function of charging voltage at low temperature for two dielectric thickness ratios. TEST 068-13R: $x_0=50$ Å, $x_n=530$ Å. TEST 067-07L: $x_0=170$ Å, $x_n=530$ Å.

[10] S. M. Hu, D. R. Kerr, and L. V. Gregor, Appl. Phys. Lett. **10**, 97 (1967).
[11] F. L. Chu, J. R. Szedon, and C. H. Lee, Solid-State Electron. **10**, 897 (1967).

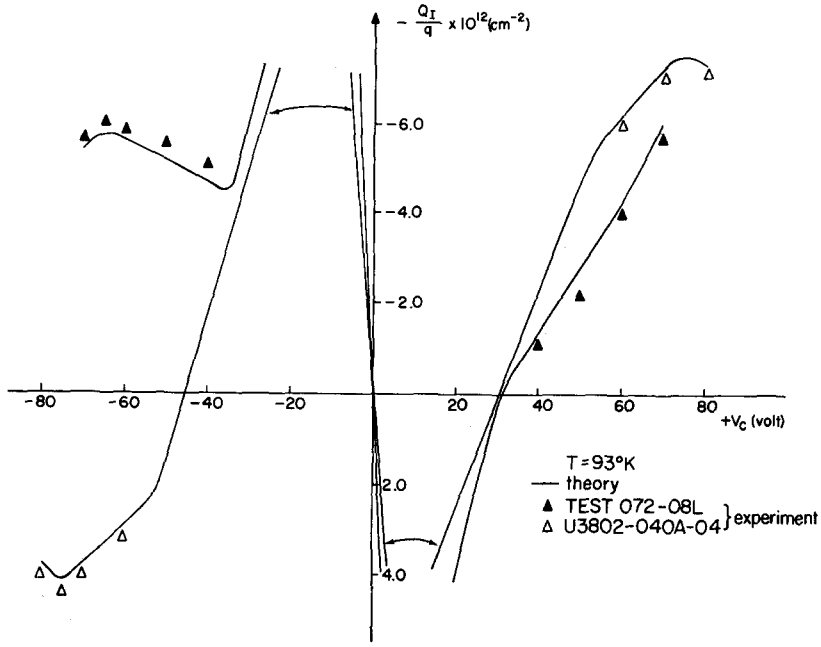

FIG. 16. Theory and experiment for the equilibrium induced interface charge as a function of charging voltage at low temperature for two values of E_2. TEST 072-08L: $x_0=50$ Å, $x_n=900$ Å, $E_2=1.28\times10^8$ V/cm. U3802-040A-04: $x_0=70$ Å, $x_n=950$ Å, $E_2=1.64\times10^8$ V/cm.

values of the initial interface charge $[Q_I(0)]$: (a) $Q_I(0)=0$, corresponding to the equilibrium condition for zero applied voltage, and (b) $Q_I(0)=-5.0\times10^{12}$ cm^{-2}, corresponding to the steady-state value of interface charge for a positive charging voltage of 50 V. If we sample the solutions at a given pulse duration t_c less than 10^6 sec, we obtain two different values of $Q_I(t_c)$ for a given value of $V_C(=40$ V).

Thus the nature of the hysteresis will be a function of both the duration of the applied charging voltage pulse (t_c) and the initial value of induced charge at the interface $Q_I(0)$. Note that for $t_c\rightarrow\infty$ both solutions merge to the steady-state value $Q_I(\infty)$, which confirms the conclusion that no hysteresis can be observed under steady-state conditions. Computer solutions of induced interface charge as a function of charging voltage for different charging times are shown in Fig. 10. To obtain solutions for the hysteresis behavior, the charging voltage was incremented from $V_{C\,\min}$ to $V_{C\,\max}$ by ΔV_C increments of duration t_c and decremented back to $V_{C\,\min}$ at the same voltage and time increments. The results for two values of t_c are shown in Fig. 11.

IV. EXPERIMENTAL PROCEDURE

Experiments were conducted with mechanically polished, n-type silicon wafers as the semiconductor

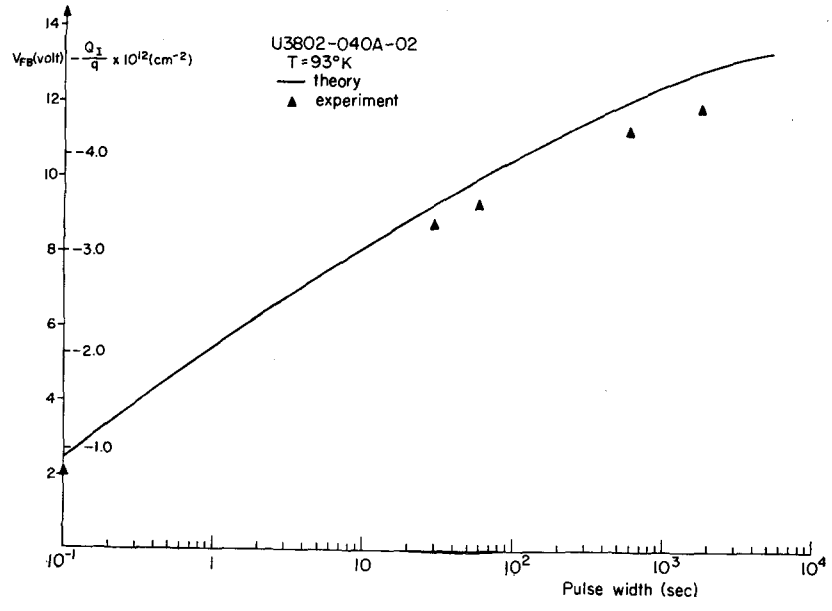

FIG. 17. Induced interface charge as a function of charging time for $V_C=+50$ V at low temperature. $x_0=70$ Å, $x_n=950$ Å, $E_2=1.64\times10^8$ V/cm.

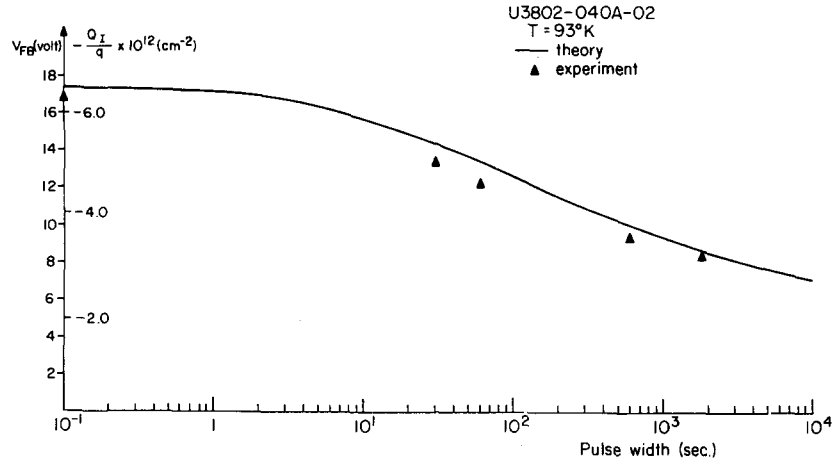

FIG. 18. Induced interface charge as a function of discharge time for $V_G = -40$ V at low temperature. $x_0 = 70$ Å, $x_n = 950$ Å, $E_2 = 1.64 \times 10^8$ V/cm.

substrate. The wafers were 200-μ thick, ⟨100⟩ oriented with a resistivity range of 5.0–8.0 Ω·cm. Thermal oxide layers of different thicknesses were grown at 920°C in a dry oxygen ambient. Silicon nitride was deposited by decomposition of $SiCl_4$ in the presence of NH_3 at 800°C, with H_2 as the carrier gas.[12] Different silicon nitride current–field characteristics were obtained by variation of the $SiCl_4$-to-NH_3 ratio.[13] In order to monitor the silicon nitride characteristics, an MNS wafer was processed in parallel with every MNOS experiment. Circular metal dots, 125-μ in diam, were defined by conventional photoresist techniques following electron-beam aluminum evaporation.

Both dielectric thicknesses were measured by a laser-beam ellipsometer and verified by interferometry techniques. The relative dielectric constant of the silicon nitride film based on capacitance measurements was found to be $K_n = 6.0$–7.5, which is consistent with results published previously.[4] The current measurements were performed with a Keithley 614B electrometer, and the accumulated interface charge Q_I was determined from capacitance–voltage measurements[7] as a shift in the flatband voltage V_{FB}. The value of fixed charge at the silicon dioxide–silicon interface Q_{ss} was typically 1.0×10^{11} cm^{-2} for all structures investigated. In all comparisons of theory and experiment, corrections were made for the small resulting shift in the flatband voltage. All current measurements were made at high applied voltages to ensure attainment of the steady-state condition for practical values of the

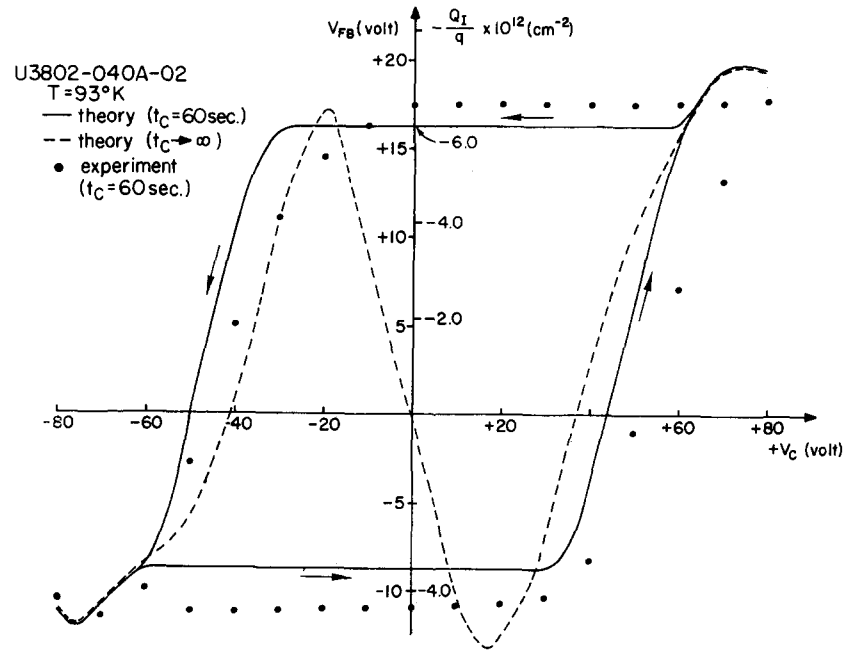

FIG. 19. Theory and experiment for the hysteresis behavior of induced interface charge as a function of charging voltage at low temperature. $x_0 = 70$ Å, $x_n = 950$ Å, $E_2 = 1.64 \times 10^8$ V/cm. The dashed line represents the theoretical steady-state solution.

[12] B. E. Deal, P. J. Fleming, and P. L. Castro, J. Electrochem. Soc. **115**, 300 (1968).
[13] G. A. Brown, W. C. Robinette, Jr., and H. G. Carlson, J. Electrochem. Soc. **115**, 948 (1968).

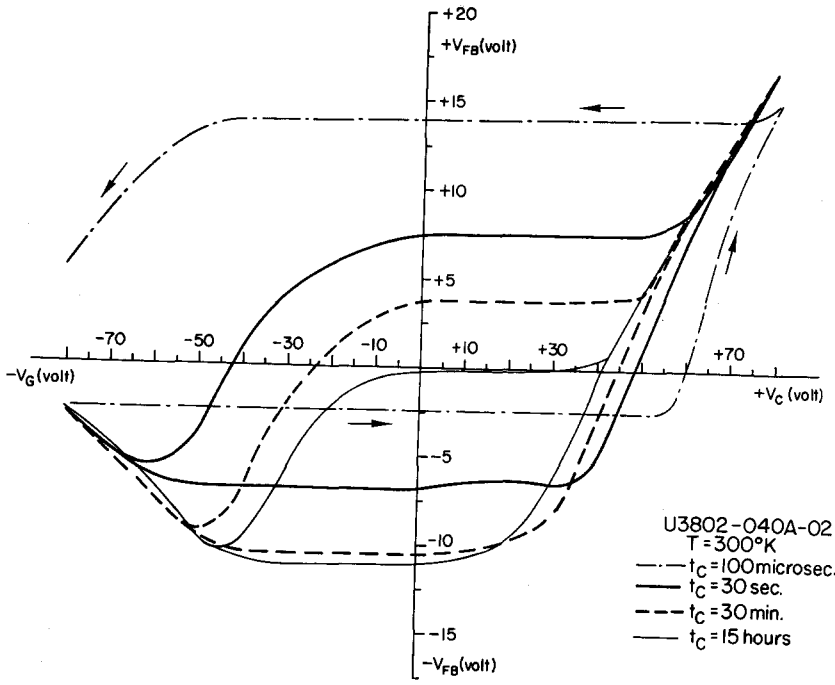

FIG. 20. Hysteresis loop of Q_I vs V_C for different values of the charging pulse, at room temperature.

charging time t_c. Since the transient analysis (Sec. III.B.) predicts a dependence of induced charge (Q_I) on the charging time (t_c), both current and flatband voltage measurements were performed after the same duration of applied charging voltage. The steady-state condition for the current was defined as the charging time beyond which the extension of pulse duration by 10 min would not change the current value by more than 10%.

V. EXPERIMENTAL RESULTS AND DISCUSSION

Presentation of the experimental results will follow the outline of the theoretical analysis in Sec. III.

A. Steady-State Current and Induced Charge

Knowledge of the characteristic parameters (e.g., ϕ_1, E_1, E_2) for the dielectric current-field relationships is required to enable a meaningful comparison of theory and experiment for the steady-state current and induced interface charge. The characteristic parameters of both silicon nitride and silicon dioxide were listed in Sec. II. These parameters were used in the comparisons between theory and experiment. In the cases when silicon nitride conduction was modified by changing deposition temperature or composition, the new parameters were determined from current-field measurements on the MNS structure processed in parallel with the MNOS capacitors. These measurements are consistent with data reported previously.[4,13]

The derivation of the theoretical model was based on the key observation that steady-state current flows through the MNOS structure. The observed steady-state current characteristics for positive and negative applied charging voltages at both room and low temperatures (liquid nitrogen) are compared with theoretical calculations for both voltage polarities in Figs. 12 and 13. The agreement in both temperature ranges is good. The corresponding calculations for the induced interface charge are compared with experimental data in Figs. 14 and 15. Comparison of induced interface charge for a structure with a different dielectric thickness ratio is also included in Fig. 15. Good agreement is obtained for both polarities. A comparison of two devices with different values of E_2 is shown in Fig. 16. Again, the agreement with theoretical calculations using independently determined values of E_2 is good. In Section III.A.1 we discussed the possibility of reversing the slope of accumulated interface charge as a function of charging voltage. This reversal is evident in Fig. 16 for negative charging voltages.

B. Time Dependence of the Induced Interface Charge

Experimental results for the induced interface charge as a function of charging time are compared in Figs. 17 and 18, with computed solutions based on Eq. (16). The agreement of both the charging (Fig. (17) and the discharging (Fig. 18) dependence on pulse duration is good. To obtain the hysteresis behavior discussed in Sec. III.B., the charging voltage was incremented from $V_{C\,\min} = -80$ V by $\Delta V = 5.0$ V increments of duration $t_c = 60$ sec up to $V_{C\,\max} = 80$ V and decremented back to $V_{C\,\min} = -80$ V at the same voltage and time increments. A comparison of the experimental hysteresis curve with that computed from Eq. (16) is shown in Fig. 19. To emphasize the departure of these characteristics from the single-line, steady-state behavior, the computed steady-state dependence is added as a

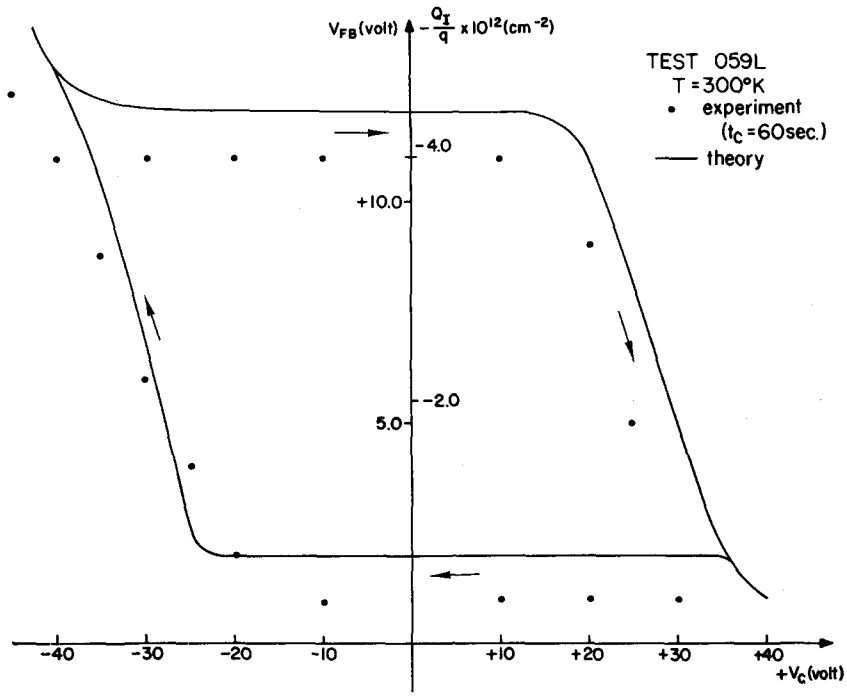

FIG. 21. Theory and experiment for the hysteresis behavior of induced interface charge as a function of charging voltage for $E_2 = 8.0 \times 10^7$ V/cm. $x_0 = 200$ Å, $x_n = 1000$ Å.

reference. Note that at high applied voltages the steady-state and transient behavior merge, while in the low-voltage range the steady-state condition cannot be achieved due to the exponential reduction in current level. To demonstrate the gradual disappearance of the hysteresis behavior as steady state is approached, the same experiment was repeated at room temperature with charging times varying from 100 μsec to 15 h. The results in Fig. 20 confirm the tendency toward a single-valued Q_I vs V_C characteristic as the duration of the charging "pulse" is increased. The hysteresis characteristics in Figs. 19 and 20 exhibit accumulation of negative charge for a positive applied voltage (conventional mode of operation). On the basis of the discussion in Sec. III.A.1, for a highly conductive nitride layer we expect the inverse mode of operation corresponding to accumulation of positive charge for a positive charging voltage. An inverse mode hysteresis characteristic obtained on a device with $E_2 = 8.0 \times 10^7$ V/cm is shown in Fig. 21 and compared with theory.

VI. CONCLUSION

A simple physical model that predicts charge accumulation at the dielectric interface of MNOS structures was proposed and verified experimentally. The model is based on the continuity of current flow in the dielectric structure. Interface-charge accumulation was shown to be determined by the requirement for continuity of current through the structure under steady-state conditions. Continuity of current is established by accumulation of either positive or negative charge for a given polarity of charging voltage, depending on the relative current-field characteristics and thicknesses of the silicon nitride and silicon dioxide layers. The accumulated interface charge dependence on temperature, oxide thickness, dielectric current-field characteristics, and charging time was predicted theoretically and shown to be in good agreement with experimental results. Due to the exponential nature of the current–field characteristics, the time required to reach steady state is a strong function of the applied charging voltage. This leads to the observed charge storage property of the MNOS device. The hysteresis characteristic observed in MNOS structures was shown to be time-dependent with a tendency to merge into a single-valued dependence of accumulated charge on charging voltage as the steady-state condition is approached. The underlying concept that charge accumulation establishes current continuity in a two-layer dielectric structure should be valid, in general, for any two-dielectric structure. Consequently, the above concept is also applicable to a thin oxide (<50 Å) MNOS structure in which direct tunneling is the dominant current-transport mechanism across the silicon dioxide layer. To obtain quantitative predictions for this structure, characterization of the direct tunneling process and knowledge of the trap distribution in the silicon nitride are required.

ACKNOWLEDGMENTS

The authors thank E. H. Snow for many helpful discussions, C. Steele for his help in processing the devices, and R. Rufford for his assistance with instrumentation and measurements.